EPJ Web of Conferences **29**, 00002 (2012)
DOI: 10.1051/epjconf/20122900002

Effect of Al-doped on physical properties of ZnO Thin films grown by spray pyrolysis on SnO_2: F/glass

M. Ajili[1,a], N. Jebbari[1], N. Kamoun Turki[1] and M. Castagné[2]

[1] Laboratoire de Physique de la Matière condensée, Faculté des Sciences de Tunis, Tunis El Manar (2092) Tunisie

[2] Institut Electronique du Sud, Université de Montpellier II, Place Eugène BATAILLON 34 095 Montpellier cedex 05 France.

Abstract. Transparent conducting thin films of aluminum-doped zinc oxide (ZnO:Al) have been deposited on SnO_2:F/glass by the chemical spray technique, starting from zinc acetate $(CH_3CO_2)_2Zn.2H_2O$ and aluminum chloride $AlCl_3$. The effect of changing the aluminum-to-zinc ratio y from 0 to 3 at.%, has been thoroughly investigated. It was found that the optical and electrical properties of Al doped ZnO films improved with the addition of aluminum in the spray solution until y=2%. At this Al doping percentage, the thin layers have a resistivity equal to 4.1 x 10^{-4} Ω.cm and a transmittance of about 90 % in the region [600-1000] nm. XRD patterns confirm that the films have polycristalline nature and a wurtzite (hexagonal) structure which characterized with (100), (002) and (101) principal orientations. The undoped films have (002) as the preferred orientation but Al doped ones have (101) as the preferred orientation. Beyond y= 1%, peak intensities decrease considerably.
Keywords. ZnO:Al, SnO_2:F, spray technique

1 Introduction

Zinc oxide (ZnO) is one of the most interesting transparent and conducting oxide (TCO) due to its electro-optical properties, high electrochemical stability, large band gap, abundance in nature and absence of toxicity. These advantages are of considerable interest for practical applications such as, gas sensors [1,2], piezoelectric devices [3], surface acoustic wave devices [4], solar cells [5-8],etc. Recently, ZnO thin films have been used as a window layer and contact layer for thin film solar cells with Cu(In,Ga)S_2 or Cu(In,Ga)Se_2 absorber material. ZnO films have been prepared by various methods of film depositions, which include radio frequency magnetron sputtering [9-11], sol–gel processing [12-16], spray pyrolysis [17,22], etc. Among these methods, the spray pyrolysis method is one of the most commonly used methods for preparation of transparent and conducting oxides owing to its simplicity, safety, non-vacuum system of deposition. Other advantage of the spray pyrolysis method is that it can be adapted easily for production of large-area films. In fact, to enhance its electrical and optical properties, ZnO is commonly doped with one of the following

[a] e-mail : ajili.mejda@yahoo.fr

elements: Indium [20], Fluorine [9], Aluminum [11-13,16-19], Gallium [14], Cobalt [15] and Tin [21]. In particular, the main reason of being chosen of aluminum as the dopant of ZnO is to enhance the electrical conductivity. When ZnO is doped Al, Al^{3+} substitutes Zn^{2+} site in the ZnO crystal structure resulting in one more free electron to contribute to the electric conduction. Furthermore, Zn can be easily substituted by Al because the aluminum radiu is smaller than that of zinc (r_{Zn}^{2+} = 0.074 nm and r_{Al}^{3+} = 0.05 nm). Al substituting Zn is therefore a good candidate as an n-type dopant in ZnO. Aluminum doped zinc oxide (AZO) grown on glass substrates was the object of our previous work [23]. It is well known that the physical properties of thin films depend on the substrate properties. Up to now, ZnO thin films were prepared on silicon, Al_2O_3, kapton, ZnO:Al, glass and sapphire substrates [9-22]. In this paper, we present the effect of aluminum dopant concentration ratio in the spray solution (y=($[Al^{3+}]/[Zn^{2+}]$)$_{solution}$= 0, 1%, 2% and 3%) on the structural, electrical and optical properties of ZnO thin layers deposited by chemical spray on nanostructured substrates such as fluorine doped tin oxide (FTO). This SnO_2: F thin layer has a thickness of about 0,6 µm and has also been deposited by spray pyrolysis on glass substrates. Our attempt will be to use AZO thin films as optical window layer in the solar cells Au/$CuInS_2$ (p)/ZnO (n)/SnO_2:F (n)/glass, where Au and SnO_2:F will be used as an ohmic contact and $CuInS_2$ as an absorber material.

2 Experimental details

Spray pyrolytic system was used to obtain FTO and aluminum doped zinc oxide (AZO) thin films. The experimental set up has been previously described [7,8]. The thin films of SnO_2:F were sprayed onto the substrate glass kept at a temperature 440°C with a spray rate of 25 ml.min^{-1}. The distance samples-nozzle is about 27 cm and the time of spray is 4 min. The solution used for pulverization consisted of tin tetrachloride ($SnCl_4$), methanol (CH_3O) and double distilled water (H_2O) [7,8]. Fluorine doping was achieved by adding fluoride NH_4F. Next, FTO samples, heated also at 440°C, are then coated by ZnO thin layers with a distance samples-nozzle of 27 cm and a spray rate of 25 ml.min^{-1}, during 40 min spray time. The spray solution consisted of zinc acetate, H_2O and propanol-2 (C_3H_8O) [7,8]. We added a few drops of acetic acid to make the solution transparent. Aluminum doping was achieved by adding aluminum chloride ($AlCl_3$).

The structure of the layers was studied by X-Ray Diffraction (XRD) which are recorded with an automated Bruker D8 advance X-Ray diffractometer with CuKα radiations for 2θ values over 20-60°. The wavelength, accelerating voltage and current were, respectively, 1.5418 Å, 40 kV and 20 mA. The morphology of the films was studied using atomic force microscopy (AFM) and scanning electron microscopy (SEM). The volume composition of AZO thin films was studied by energy dispersive spectrometry (EDS) coupled with (SEM). Resistivity, surface and volume carrier concentration and mobility were determined from Hall effect measurements in the Van der Paw-configuration. The optical properties were studied according to UV-VIS-NIR spectrum with a Perkin–Elmer Lambda 950 spectrophotometer in the wavelength range of 250-2500 nm at room temperature, taking the air as reference. The average grain size D is estimated by the scherrer's formula [24]:

$$D = \frac{0.9 \times \lambda}{B \cos\theta} \quad (1)$$

Where λ is the X-ray wavelength of CuKα radiation (λ= 1.54 Å), B is the full-width at half-maximum (FWHM) of the diffraction in radians and θ is the Bragg diffraction angle.

3 Results and discussion

3.1 Structural analysis

3.1.1 X-Ray Diffraction

In order to study the effect of aluminum concentration on the microstructural properties of AZO thin layers deposited on SnO_2:F/Glass. The XRD patterns of four films grown for different doping concentrations are shown in Figure 1. The spectra show a polycristalline character with the typical hexagonal wurtzite structure for ZnO, though the preferential orientation changes with adding aluminum to the spray solution. The same behaviour was observed by Amlouk and al [20] and M. De la L. Olvera and al [18]. The undoped films have (002) preferred orientation. Secondary peaks are (100), (101), (102) and (110) with two peaks (200) and (211) correspond to the SnO_2:F thin layers. For y=1%, the intensity of (002) orientation decreases, the (100) and (101) peak intensities increase and the principal orientation becomes (101). In contrast, when y=2% or 3%, the film undergoes a dramatic change: the AZO thin films become clearly less oriented, with a resulting sharp decrease in the (002) and (101) peak intensity. The same thin layers deposited on glass substrates have the highest (002) diffraction peak intensity indicating that (002) is the preferential orientation which its intensity increased with increasing the y ratio until 2%, but if y=3% this intensity decreased [23]. This revealed that the structural properties of AZO depend on the used substrate.

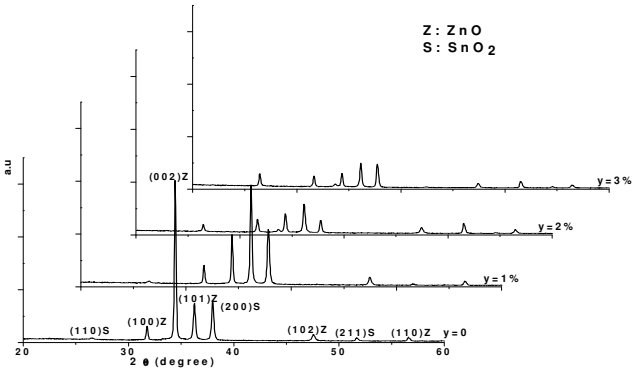

Fig. 1. X-Ray Diffraction of AZO thin layers grown on SnO_2:F/glass substrate at different aluminum doping concentrations (y= $[Al^{3+}]/[Zn^{2+}]$). Peaks corresponding to FTO and AZO compound are respectively indexed by Z and S.

The incorporation of aluminum atoms into zinc oxide films influences the film thicknesses “e” as shown in Figure 2. For undoped films, the thickness is in the order of 1.86 µm. AZO thin films grown for y= 1% have 1.34 µm thickness then e decreases to 0.85 and 0.64 µm respectively for y= 2% and 3%. When the doping is equal to 1 at.%, 2 at.% and 3 at.%, the (002) peak intensity decreases respectively by a factor of 0.33, 0.18 and 0.17 with the respect to the undoped layer. The film thickness decreases also respectively by a factor of 0.72, 0.46 and 0.34. So, this disparity between the decrease in the peak intensity and the decrease in the film thickness, clearly indicates that the changes observed in the diffractograms are indeed the results of structural changes caused by the aluminum doping and not only by the variation in the film thickness. Similar results is obtained by J. L. Van Heerden and al [25].

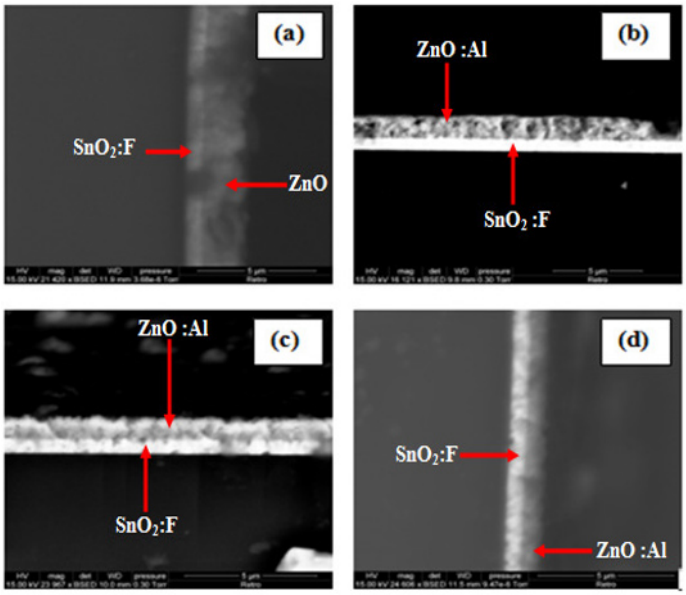

Fi g. 2. Cross-sectional SEM micrograph of AZO thin films grown on SnO_2:F/glass subtrate at different aluminum doping concentrations in the spray solution (y= $[Al^{3+}]/[Zn^{2+}]$) : (a) : y= 0, (b) : y= 1%, (c) : y= 2% and (d) : y= 3%.

3.1.2 Surface morphology

AFM images of AZO thin films deposited on SnO_2:F/glass are illustrated in Figure.3. All films surfaces show a rough texture, and numerous porous surrounding the grains can be evidenced.The undoped and 1 at.% Al doped samples show aggregated grains with spherical shape when compared to the 2 and 3 at. % Al doped ones. The 2 at. % Al doped thin layers have irregular shape of grains. This result can leads to more grain boundaries in these layers. For y reached 3% grains become of elongated shape.

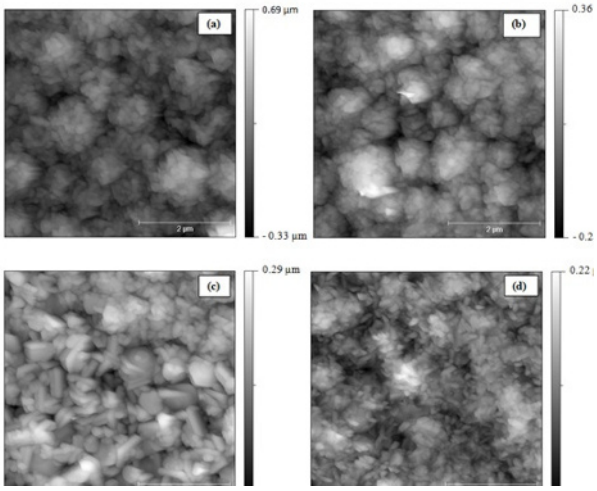

Fig. 3. Surface topography of AZO thin films grown on SnO_2:F/glass subtrate at different aluminum doping concentrations ((y= $[Al^{3+}]/[Zn^{2+}]$) (a): y= 0, (b): y= 1%, (c): y= 2% and (d): y= 3%).

Table 1 present the variance of height distribution (RMS roughness) calculated from AFM images and the mean grain size (D) calculated from Scherrer's formula. We notice that an increase of the dopant concentration reduced the grain size. This result is in agreement with that found by K. Y. Cheong and al [14]. Indeed, this gradual decrease of D may be attributed to the increasing number of centers during incorporation of the doping into the host material. In addition, we remark that the RMS roughness decreases by increasing the aluminum doping concentration.

Table 1. RMS roughness and mean grain (D) size of AZO thin layers elaborated on SnO_2:F/glass subtrate at different aluminum doping concentrations (y= $[Al^{3+}]/[Zn^{2+}]$= 0, 1%, 2% and 3%).

y	RMS (nm)	D (nm)
0	112	45
1%	91	42
2%	83	39
3%	53	33

3.2 Volume-chemical composition

Measurements of the atomic concentration are taken at different position of the samples by EDS. The average value in atomic percent of each element in AZO material grown at different concentrations of aluminum dopant is presented in Table. 2. It is clear that aluminum dopant concentration influences the volume composition of the AZO thin layers. The atomic concentration of Al in the solid is close to the spray solution one. This result shows the spray advantage in the conservation of ionic ratio after deposition. Thus, for y= 0 to 1%, the atomic percent of O decreases but it increases for Zn. However, for y= 2% and y= 3% the atomic percent of O increases and it decreases for Zn. This can be correlated with the structural analysis performed by X-Ray Diffraction which shows that the crystallization is worse for y= 2% and y=3% compared with 1 at.% Al doped samples. The average value of [Zn]/ [O] in the ZnO/SnO_2:F/glass thin layer varies with the ratio y in the spray solution and for y= 1%, this value is around the stochiometer values. In fact, the best volume-chemical composition of AZO thin films was obtained for 1 at. % Al doped ones. On the other hand, the average value of [Zn]/ [O] of all AZO thin layers deposited on glass substrates is around of stochiometer values [23]. So, the volume-chemical composition of AZO thin films depends also on the substrate.

Table 2. EDS analyses of AZO thin layers grown on SnO_2:F/glass substrate at different aluminum doping concentrations (y= $[Al^{3+}]/[Zn^{2+}]$= 0, 1%, 2% and 3%).

y	O (%)	Zn (%)	Al (%)	[Zn]/[O]	[Al]/[Zn] (%)
0	63.67	36.33	0	0.57	0
1%	53.24	46.31	0.46	0.87	0.99

2%	59.7	40	0.7	0.67	1,75
3%	60.67	38.36	0.97	0.63	2.52

3.3 Optical properties

In order to study the effect of aluminum concentration on the optical properties, we plotted in Figure 4, the optical transmission and reflection of AZO thin films grown for different values of y. One can observe that the optical transmittance spectra of ZnO:Al films represent a strong dependence with the aluminum doping. The average transmittance in the region [600-1000] nm is about 90% when the concentration of Al dopant is 1 or 2 at. %. This value indicates a good quality of AZO material with high transparency of layers, predisposing them to be used as an optical window in visible range in photovoltaic systems. Beyond y=2%, the transmittance decreases remarkably. The undulating shape of the transmission curves is caused by interference of the light in the film itself. This result is similar for tin doped zinc oxide elaborated by a two-stage chemical deposition (TSCD) [21]. Besides we note the presence of the interference fringes characteristics of fairly uniform in thickness and quite homogenous layers in accordance with the morphological study. Similar results was previously reported [20,22]. Moreover, for all aluminum doping concentration and in the region of intrinsic absorption edge of ZnO, we note the existence of a slight shoulder in the spectrum of T(λ) which may correspond to an excitonic peak in the compound AZO whose amplitude varies with the value of y. This shoulder reaches its maximum for y= 1%, it may be due to the fact that the 1 at. % aluminum doped zinc oxide thin layer is very homogenous and has good optical characterization.

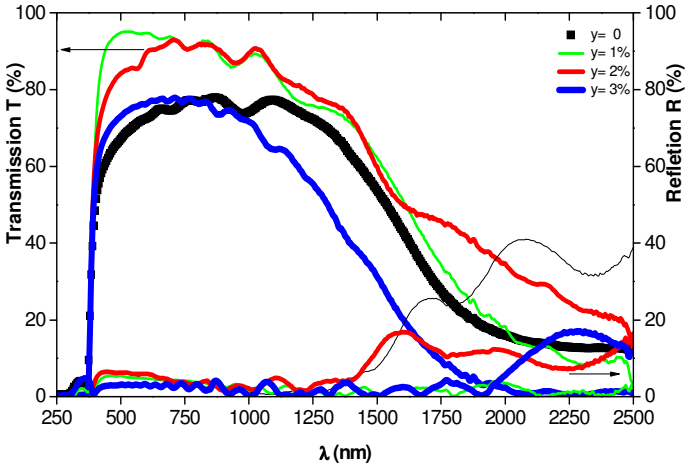

Fig. 5. Transmission and reflection spectra of AZO thin films deposited on SnO_2:F/glass substrates at different aluminum doping concentrations (y= $[Al^{3+}]/[Zn^{2+}]$).

As a direct band gap semiconductor, the band of ZnO film is an important parameter. According the following formula, the band gap depend on the optical absorption coefficient and the photon energy hυ [26]:

$$(\alpha h\upsilon) = A\,(h\upsilon - E_g)^n \qquad (2)$$

Where A is a constant, h is planck's constant, υ is the photon frequency, E_g is the optical band gap, n is ½ for direct band gap and α is the absorption coefficient, which can be calculated from the film thickness e, transmittance T and reflectance R measurements by using the formula [27] :

$$\alpha = -\frac{1}{e} Ln[\frac{T}{(1-R)^2}] \quad (3)$$

Figure 6 shows variations of $(\alpha h\upsilon)^2$ vs. Photon energy hυ for pure ZnO and ZnO :Al (y= 1%, 2% and 3%). The linear part of the curves for high photon energies indicates that the ZnO :Al films are essentially semiconductors with direct-transtion-type. Extrapolation of the linear portions of $(\alpha h\upsilon)^2$ to zero gave the value of E_g. The estimated E_g values for ZnO:Al films are 3.26, 3.22, 3.21 and 3.25 eV for y= 0, 1%, 2% and 3% respectively. Thus, it can be concluded that Al as a dopant of ZnO/SnO_2:F/Glass thin films does not contribute any significant changes to the optical band gap of the film.

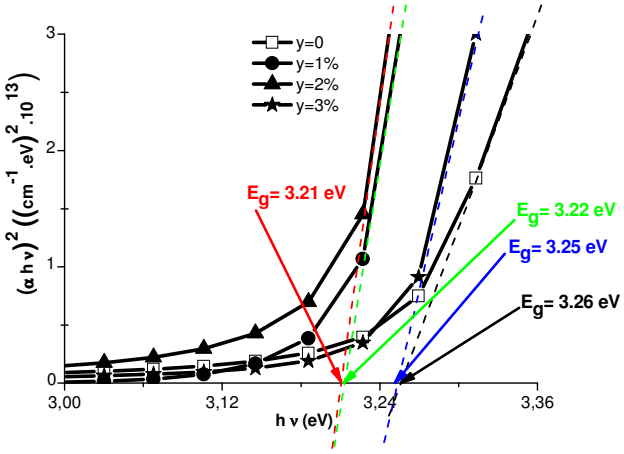

Figure 6. Variation $(\alpha h\upsilon)^2 = f(h\upsilon)$ of AZO thin films deposited on SnO_2:F/glass substrates at different aluminum doping concentrations (y= $[Al^{3+}]/[Zn^{2+}]$).

3. 4 Electrical properties

It is well admitted that conduction properties of ZnO are primarily dominated by electrons generated from O^{2-} vacancies and Zn^{2+} intertitial atoms. The electrical conductivity in ZnO:Al thin films is higher than that of undoped ZnO films, it may be due to the contribution of Al^{3+} ions on substitutional sites of Zn^{2+} ions, as it has been shown by other autors [13,19]. All our Hall measurement results are listed in table 3. It is shown that aluminum dopant is the most important parameter that affects the electrical properties of AZO thin films, as evidenced by table 3. The resistivity decreases sharply with dopant quantity, it is in the order of 5.8 10^{-4} and 4.1 x 10^{-4} Ω.cm for y equal to 1 and 2, respectively and then it increases. The minimum resistivity of as-deposited AZO on SnO_2:F/glass is more lower compared with those doped also with 1 and 2 at. % Al deposited on glass where whose value is in the order of 1.3 and 1.5 Ω.cm for y equal to 1 and 2%, respectively [23]. Thus, the electrical resistivity of AZO depends strongly on the substrate at which AZO thin layers were deposited. The decrease in the resistivity of the films by aluminum doping can be explained by the substitution of Al^{3+} ions at the Zn^{2+} sites leading one free carrier, as reported earlier [13,19]. As the doping levels increased, more dopant atoms occupy the zinc lattices sites, which results in more charge carriers. This process continues as long as the zinc sites are available. However, after a certain level of doping, the Al atoms cannot occupy lattices sites and they have a

tendency to occupy interstitial sites where they form neutral defects and become ineffective as dopant impurities. So, it is apparent from table 3, that the surface and volume charge carrier concentration (N_s and N_v) of the films show a gradual increase with the increase of aluminum dopant concentration until the value of 2 %, reaching repectively 21.03 x 10^{17} cm^{-2} and 24.42 x 10^{21} cm^{-3}. Above 2%, N_s and N_v show sudden decrease. In contrast, the Hall mobility μ is decreasing (table 3) with increase the aluminum dopant concentration. Above 2% μ increases. The maximum value of μ is 120.8 $cm^2.V^{-1}$ for the undoped thin layers. N_s and N_v are higher for y = 2% than y=1% but the mobility is slightly higher for y = 1%. This result can be correlated by the AFM analysis which showed that for 2at. % AZO thin layers, there is more grain boundaries than that for 1at. % ones.

Table 3. Hall data of AZO thin layers deposited on SnO_2:F grown at different Aluminum doping concentrations (y= $[Al^{3+}]/[Zn^{2+}]$= 0, 1%, 2% and 3%).

y (%)	ρ (x 10^{-4} Ω.cm)	N_s (x 10^{17} cm^2)	N_v (x 10^{21} cm^{-3})	μ ($cm^2.V^{-1}$)
0	13.3	0.15	0.11	120.8
1	5.8	8.91	8.23	2.9
2	4.1	21.03	24.42	2.3
3	16.7	1.09	1.52	7.9

4 Conclusion

In summary, the AZO thin films have been deposited on SnO_2:F/glass by the spray pyrolysis technique. The introduction of Al dopant can alter the film structure and affect the growth of AZO thin films because the thickness of these thin layers vary when we change the amount of aluminum introduced into the spray solution. On the other hand, the incorporation of this dopant reduce the grain size and surface roughness. The improvement in the electrical and optical properties was obtained for AZO thin films grown at y equals to 1%. The best optical transmittance were also achieved by ZnO film doped with 1 at. % Al. This will allow us to use 1 at. % aluminum doped zinc oxide thin films as optical window in photovoltaic cell such as Au/$CuInS_2$/AZO/SnO_2:F where the growth by spray of SnO_2:F et $CuInS_2$ thin films is well controlled in our laboratory [7,8,28,29]. In perspective to optimize the performance of ZnO i.e good cristalinity, tranparent and conducting films, the study of the influence of tin dopant on the physical characteristics of chemically sprayed ZnO is in the course of realization.

References

1. M.-W. Ahn, K.-S. Park, J. Heo, D.-W. Kim, K.J.Choi, J,-G. Park, Sensors and Actuators B **138** (2009) 168-173.
2. Kuwei Liu, Makoto Sakurai, Masakazu Aono, Sensors and Actuators B **157** (2011) 98-102.
3. S.H. Jeong, B.N. Park, S.-B. Lee, J,-H. Boo, Thin Solid Films, **516** (2008) 5586-5589.
4. Tsung-Tsong Wu and Wei-Shan Wang, Journal of Applied Physics, 96 number **9** (2004) 5249-5253.
5. B. Asengo, A.M. Chaparro, M.T. Gutierrez, J. Herrero, J. Klaer, Solar Energy Materials and solar cells **87** (2005) 647-656.
6. M. Krunks, A.Katerski, T. Dedova, I. Oja Acik, A; Mere, Solar Energy Materials and Solar Cells **92** (2008) 1016-1019.

7. N. Jebbari, B. Ouertani, M. Ramonda, C. Guasch, N. Kamoun Turki and R. Bennaceur, Energy Procedia **2** (2010) 79-89.
8. N. Kamoun Allouche, T. Ben Nasr, N. Kamoun Turki and M. Castagne, Energy Procedia **2** (2010) 91-101.
9. Yu-Zen Tsai, Na-Fu Wang, Chun-Lung Tsai, Thin Solid films **518** (2010) 4955-4959.
10. Petronela Prepelita, R. Medianu, Beatrice Sbarcea, F. Garoi, Mihaela Filipescu, Applied surface science **256** (2010) 1807-1811.
11. J.J Ding, H.X. Chen, S. Y. Ma, Applied surface science, **256** (2010) 4304-4309.
12. S. W. Xue, X. T. Zu, W.G. Zheng, M. Y. Chen, X. Xiang, Physica B **382** (2006) 201-204.
13. Xu Zi-qiang, Deng Hong, Li Yang, Cheng Hang,Materials Science in Semiconductor Processing **9** (2006) 132-135.
14. K. Y. Cheong, Norani Muti, S. Ramanan, Thin Solid Films **410** (2002) 142-146.
15. Nupur Bahadur, A.K. Srivastava, Sushil Kumar, M. Deepa, Bhavya Nag, Thin Solid Films **518** (2010) 5257-5264.
16. Young-Sung Kim, Weon-Pil Tai, Applied Surface Science **253** (2007) 4911-4916.
17. H. Mondragon -Suarez, A. Maldonado, M. De la L. Olvera, A. Reyes, R. Castanedo-Pérez, G. Torres-Delgado, R. Asomozo, Applied Surface Science **193** (2002) 52-59.
18. M. de la L. Olveraa, A. Maldonadoa, J. Vega-Péreza, O. Solorza-Feriab, Materials Science and Engineering B **174** (2010) 42–45.
19. L. Castaneda, R. Silva-Gonzalez, J. M. Gracia-Jiménez, M. E. Hernandez-Torres, M. Avendano-Alejo, César Marquez-Beltran, M. De la L. Vega-Pérez, A. Maldonado, Materials Science in Semiconductor Processing **13** (2010) 80-85.
20. M. Amlouk, S. Belgacem, N. Kamoun, H. Elhouichet, R. Bennaceur, Semi-Conductors and thin films, Ann. Chim. Fr., 1994, **19**, pp. 469-472.
21. M. R. Vaezi, S. K. Sadnezhaad, Materaials Sciences and Engineering B **141** (2007).
22. M. Mekhnache, A. Drici, L. Saad Hamideche, H. Benzarouk, A. Amara, L. Cattin, J. C. Bernède, M. Guerioune, Superlattices and Microstructures **49** (2011) 510-518.
23. M. Ajili, N. Jebbari, N. Kamoun Turki, M. Castagné, **IREC**, November 5- 7, 2010-Sousse, Tunisa.
24. Buerger MJ (1960) X- ray crystallography. Wiley, New York, p 23.
25. J.L. van Heerden, R. Swanepoel, Thin Solid Films **299** (1997) 72-77.
26. M. Girtan, G. Folcher, Surf. Coat. Technol. **172** (2003) 242.
27. S. Belgacem et R. Bennaceur, Revue Phys. Appl. **25** (1990) 1245-1258.
28. N. Kamoun, R. Bennaceur et J. M. Frigerio, J. Phys. III France **4** (1994) 983-996.
29. N. Kamoun, N. Jebbari, S. Belgacem, and R. Bennaceur, Journal of Applied Physics **91** (2002) 1952-1955.